THE JOURNAL OF BIOLOGICAL CHEMISTRY VOL. 288, NO. 15, pp. 10265–10274, April 12, 2013

Endothelial Cell-specific Chemotaxis Receptor (ECSCR) Enhances Vascular Endothelial Growth Factor (VEGF) Receptor-2/Kinase Insert Domain Receptor (KDR) Activation and Promotes Proteolysis of Internalized KDR*[S]

Received for publication, August 24, 2012, and in revised form, February 1, 2013 Published, JBC Papers in Press, February 7, 2013, DOI 10.1074/jbc.M112.413542

Sreenivasulu Kilari[‡], Indulekha Remadevi[‡], Baofeng Zhao[§], Jing Pan[¶], Robert Miao[§], Ramani Ramchandran[‡], Paula E. North[‖], Ming You[¶], Nader Rahimi[**], and George A. Wilkinson[‡1]

From the [‡]Department of Pediatrics and Developmental Vascular Biology Program, [§]Divisions of Pediatric Surgery and Pediatric Pathology and Departments of Surgery and Pathology, Departments of [¶]Pharmacology and Toxicology and [‖]Pathology and Laboratory Medicine, Medical College of Wisconsin and Children's Research Institute, Milwaukee, Wisconsin 53226 and [**]Departments of Pathology and Ophthalmology, Boston University Medical School, Boston, Massachusetts 02118

Background: ECSCR is required for full KDR activation, but the mechanism is unknown.
Results: ECSCR and KDR show both basal and VEGF-stimulated association.
Conclusion: ECSCR modulates KDR activation and proteolysis of internalized KDR.
Significance: ECSCR expression in vascular anomalies such as infantile hemangioma has implications for VEGF signaling in those tissues. In contrast, ECSCR levels are not increased in lung squamous cell carcinoma.

The endothelial cell-specific chemotaxis receptor (ECSCR) is a cell-surface protein selectively expressed by endothelial cells (ECs), with roles in EC migration, apoptosis and proliferation. Our previous study (Verma, A., Bhattacharya, R., Remadevi, I., Li, K., Pramanik, K., Samant, G. V., Horswill, M., Chun, C. Z., Zhao, B., Wang, E., Miao, R. Q., Mukhopadhyay, D., Ramchandran, R., and Wilkinson, G. A. (2010) *Blood* 115, 4614–4622) showed that loss of ECSCR in primary ECs reduced tyrosine phosphorylation of vascular endothelial growth factor (VEGF) receptor 2/kinase insert domain receptor (KDR) but not VEGF receptor 1/FLT1. Here, we show that ECSCR biochemically associates with KDR but not FLT1 and that the predicted ECSCR cytoplasmic and transmembrane regions can each confer association with KDR. Stimulation with $VEGF_{165}$ rapidly and transiently increases ECSCR-KDR complex formation, a process blocked by the KDR tyrosine kinase inhibitor compound SU5416 or inhibitors of endosomal acidification. Triple labeling experiments show VEGF-stimulated $KDR^+/ECSCR^+$ intracellular co-localization. Silencing of ECSCR disrupts VEGF-induced KDR activation and AKT and ERK phosphorylation and impairs VEGF-stimulated KDR degradation. In zebrafish, *ecscr* interacts with *kdrl* during intersomitic vessel sprouting. Human placenta and infantile hemangioma samples highly express ECSCR protein, suggesting a role for ECSCR-KDR interaction in these tissues.

Vascular endothelial growth factor (VEGF) and its receptors are key regulators of endothelial cell biology, influencing differentiation, survival, proliferation, and migration of endothelial cells. VEGF is produced in isoforms of varying amino acid chain lengths, of which the two most abundant isoforms, $VEGF_{121}$ and $VEGF_{165}$, show distinct binding and biological activities. At least part of this difference can be explained by their relative activity toward the VEGF co-receptor neuropilin-1 (NRP1)[2]. $VEGF_{165}$ but not $VEGF_{121}$ binding to VEGF receptor-2 (also known as KDR) promotes stable complex formation with the coreceptor NRP1 (Refs. 2 and 3).

Recent studies have shed light on the intricate routing of internalized KDR following VEGF stimulation (reviewed in Refs. 4 and 5). In resting cells, a substantial fraction of KDR receptor resides in intracellular pools in exchange with the cell surface (6). VEGF stimulation results in KDR internalization and trafficking, toward recycling endosomes identified by the small GTPase RAB11, or toward a degradative pathway marked by the small GTPase RAB7. NRP1 engagement by VEGF is a key influence on KDR intracellular routing (7) and VEGF isoforms that do not bind NRP-1 favor routing of KDR toward proteolysis (7). VEGF stimulation also elicits KDR ubiquitination (8) and increases KDR association with hepatocyte growth factor-regulated substrate (HRS; 9), a component of the ESCRT (endosomal sorting complex required for transport), which recognizes and sorts internalized ubiquitinated receptors (reviewed in Ref. 10).

Endothelial cell-specific chemotaxis receptor (ECSCR), also known as ECSM2 and apoptosis regulator through modulating IAP expression (ARIA), was initially identified (11, 12) as a novel mRNA preferentially expressed in endothelial cells, which encoded a cell-surface single-transmembrane domain

* This work was supported by Children's Research Institute startup funds and American Heart Association Scientist Development Grant 11SDG5310020 (to G. A. W.).
[S] This article contains supplemental Table 1 and Figs. 1–6.
[1] To whom correspondence should be addressed: Developmental Vascular Biology Program, TBRC/CRI C-3415, 8701 Watertown Plank Rd., Milwaukee, WI 53226. Tel.: 414-955-2389; Fax: 414-955-6325; E-mail: gwilkins@mcw.edu.

[2] The abbreviations used are: NRP1, neuropilin-1; EC, endothelial cell; ECSCR, endothelial cell-specific chemotaxis receptor; KDR, kinase insert domain receptor; HRS, hepatocyte growth factor-regulated substrate; ISV, intersomitic vessel; HUVEC, human umbilical vein endothelial cell; PAE, porcine aortic endothelial; MO, morpholino.

glycoprotein (13) with highly conserved transmembrane and cytoplasmic sequences. The cytoplasmic domain interacts with the actin-binding protein filamin-A (11), the proteasome (14), and phosphatase and tensin homologue (15), whereas the binding properties of the transmembrane region are unknown. ECSCR function has been implicated in cell migration, angiogenesis, and apoptosis (reviewed in Ref. 16).

In our previous work (1), we showed that ECs silenced for *ECSCR* manifest reduced VEGF-induced migration and reduced tyrosine phosphorylation of KDR but not of VEGF receptor 1 (FLT1). However, the mechanism by which ECSCR influences KDR activation, and the sequence determinants of this function are unknown. In this work, we provide evidence that ECSCR associates biochemically with KDR and that lack of ECSCR impairs VEGF-stimulated KDR activation, signaling, and proteolysis. These data suggest two distinct roles for KDR/ECSCR association: in resting cells, basal association increases KDR activation, whereas a delayed association in stimulated cells enhances KDR degradation.

EXPERIMENTAL PROCEDURES

Antisera and Reagents—Anti-V5 and anti-Myc-tag antisera were from Invitrogen. The antibodies to FLT1, NRP1, mouse anti-KDR, and phospho-KDR (Tyr^{951}) were from Santa Cruz Biotechnology. Antibodies against RAB7 and RAB11, phospho-KDR (Tyr^{1175}), rabbit anti-KDR, total and phospho-p42/44 ERK, and total and (phospho-Ser^{473}) AKT were from Cell Signaling. Anti-HRS was from Enzo Life Sciences. Alexa Fluor 633-coupled Ulex-1 lectin, recognizing human endothelial cells, was from Invitrogen.

KDR kinase inhibitor III SU5416 was from Calbiochem. Src family kinase inhibitor PP2 was from Tocris. Chloroquine diphosphate and bafilomycin A1 were from Sigma. $VEGF_{165}$ and $VEGF_{121}$ were from Peprotech. Polyclonal anti-ECSCR antiserum was raised in rabbits immunized using a GST fusion with the human ECSCR C terminus as an antigen. Biochemistry assays, including immunoprecipitation and Western blot were performed as described (1) with the exception that the base buffer used was radioimmune precipitation assay buffer (Sigma) to improve stringency of co-immunoprecipitation. siRNAs targeting ECSCR were from Qiagen (SI04328177) and from Sigma (SASI_Hs02_00313147).

ECSCR Structure/Function Constructs—Recombinant constructs were designed based on human ECSCR (GenBank™ accession no. NP_001071161) and human endomucin (EMCN) (GenBank™ accession no. NP_001153166), with chimeric constructs conforming to annotated transmembrane region boundaries. ECSCR-ΔC specifies the ECSCR sequence up to residue Glu^{165}.

Zebrafish—All zebrafish studies were performed under the Medical College of Wisconsin institutional guidelines (Animal Protocol 312-06-2). *Kdrl:eGFP* transgenic fish (17) were crossed, and eggs were injected with morpholinos against *ecscr* (MO3; 1) and/or *kdrl* (ATG MO; 18). Fish were scored for intersomitic vessel sprouting at 22 hours post-fertilization (hpf). Additive effects on intersomitic vessel (ISV) sprouting following injection of MO mixtures were evaluated as described (19).

Human Patient Samples—Research on human patient samples was performed according to Medical College of Wisconsin-approved Institutional Review Board protocols, and informed consent was obtained in accordance with the Declaration of Helsinki. Tissue array CVD481 was obtained from U. S. Biomax.

Cell Culture—Endothelial cells were maintained on tissue culture plastic unless indicated otherwise. HUVECs were purchased from Lonza and cultured in endothelial basal medium-2 plus endothelial supplements (Lonza) for four to six passages. Porcine aortic endothelial (PAE) cells and transduced lines were maintained in F11 + penicillin/streptomycin/glutamine plus 10% FBS. Transfection of both cell types was performed by lipofection for biochemistry. For immunocytochemistry, HUVECs were microporated using the Neon transfection system (Invitrogen). siRNA transfection of HUVEC cells was performed at 80% confluence using oligofectamine reagent (Invitrogen) (20).

Motility of KDR-PAE Cells—Cell migration was measured in Boyden chambers with 8-μm pore inserts. Cells were transiently transfected with indicated constructs, resuspended in serum-free media, and starved for 1–2 h before the assay. Boyden chambers were placed over a lower chamber containing or purified $VEGF_{165}$ (25 ng/ml) in endothelial basal medium. Upper chambers were seeded at a density of 2×10^4 cells per well in 500 μl of serum-free media. Cells were allowed to migrate for 5 h at 37 °C in 5% CO_2. Migration experiments were repeated in their entirety at least twice.

Cell Fractionation and Differential Centrifugation—Serum-starved or VEGF stimulated HUVECs were monolayers washed with ice-cold PBS and collected by scraping. Cells were resuspended in hypotonic buffer (20 mM Tris-HCl, pH. 8.0, containing 10 mM KCl, 0.2 mM $MgCl_2$, and protease and phosphatase inhibitors), and lysed by passing through a 26-gauge needle. Lysates were clarified thrice by centrifugation at 300 × *g* for 10 min. Clarified lysates were subjected to centrifugation at 1000 × *g* for 10 min to pellet nucleus and plasma membrane (low-speed pellet; fraction 1). The low speed supernatant was subjected to medium speed centrifugation at 30,000 × *g* for 30 min to enrich for endosomes (medium speed pellet; fraction 2). Finally, other membranes were pelleted by ultracentrifugation at 100,000 × *g* for 1 h (fraction 3), with the supernatant (fraction 4) enriched in cytosol. 30 μg of protein fractions were resolved on 4–20% gradient SDS-PAGE followed by immunoblotting. Prep quality was monitored by blotting fractions for membrane-associated Na^+/K^+ ATPase and for cytosolic GAPDH.

RESULTS

ECSCR Biochemically Associates with KDR—Because our earlier data (1) indicated that loss of ECSCR affected VEGF-stimulated KDR tyrosine phosphorylation, we asked whether these two proteins associate biochemically (Fig. 1). We co-transfected HEK293 cells with KDR and either tagged ECSCR (ECSCR-FL) or a truncation mutant lacking most of the conserved cytoplasmic domain (ECSCR-ΔC; sequence details given in "Experimental Procedures"). Anti-tag immunoprecipitation (IP) showed robust association of endogenous KDR with ECSCR-FL and -ΔC (Fig. 1*A*). Reverse IP also showed both FL

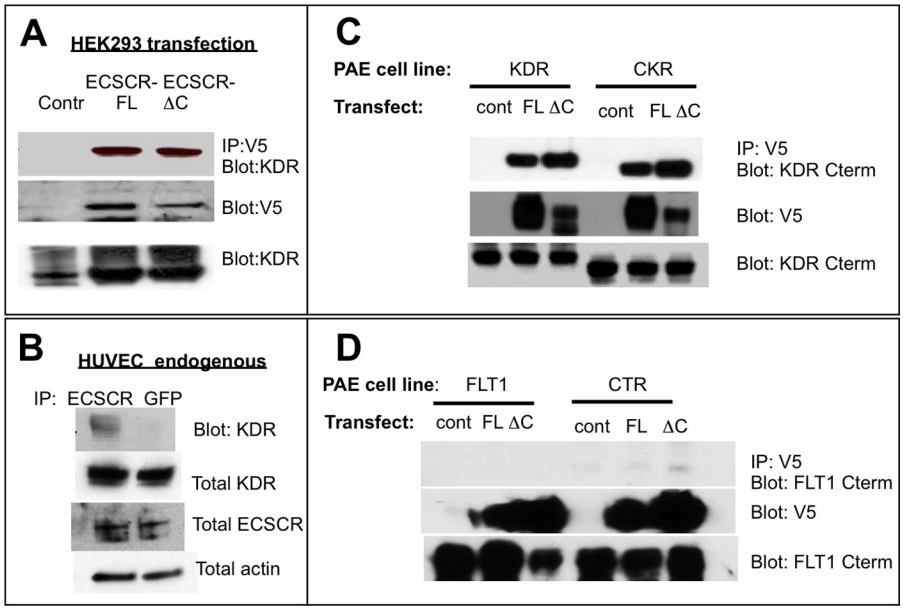

FIGURE 1. **Mutually selective association of KDR with ECSCR.** *A*, HUVECs were transfected with tagged ECSCR full-length (*ECSCR-FL*) or cytoplasmic-truncated (*ECSCR-ΔC*) constructs. Cell lysates were subjected to anti-tag immunoprecipitation and probed by anti-endogenous KDR Western blot. KDR is detected in both immunoprecipitates but not in control. *B*, KDR is also detected in HUVECs immunoprecipitated with anti-endogenous ECSCR but not control antiserum. *C*, PAE cells transduced with wild-type KDR or a chimeric receptor containing CSF-1R extracellular sequences (see text) both co-IP with ECSCR or with ECSCR-ΔC. *D*, in transduced PAE lines, neither FLT1 nor chimeric CSF-1R/FLT receptor show co-IP with ECSCR. *cont*, control.

and ΔC ECSCR in anti-KDR immunoprecipitates (data not shown). To address whether endogenous ECSCR can associate with endogenous KDR, we raised and affinity-purified antiserum against the conserved carboxyterminal portion of human ECSCR. Immunoprecipitates using anti-endogenous ECSCR, but not control antiserum, co-precipitated endogenous KDR from HUVEC lysates (Fig. 1*B*).

To understand the degree of selectivity of ECSCR-KDR interaction, and to begin to map the sequence determinants by which ECSCR and KDR interact, we analyzed chimeric receptor molecules in a PAE cell transfection system. PAE cells express very low levels of VEGF binding co-receptors (21) and can be used to study VEGF receptors in relative isolation. We transfected ECSCR and derivative constructs into PAE lines singly transduced with KDR; with VEGF receptor 1 (FLT1); or with chimeric CKR or CTR constructs (containing CSF-1R extracellular domain and KDR or FLT1 transmembrane and cytoplasmic domains, respectively; Ref. 22). Anti-tag IP of ECSCR-FL or -ΔC in PAE lines co-precipitated KDR and CKR chimeric receptor (Fig. 1*C*). In contrast, we did not detect association of ECSCR-FL or -ΔC with FLT1 or with chimeric CTR (Fig. 1*D*). As CKR but not CTR was detected in ECSCR immunoprecipitates, we infer that the CSF-1R extracellular domain, shared by the CTR and CKR chimeras, did not contribute detectably to association between ECSCR and CKR. We have not detected binding between recombinant soluble ECSCR extracellular domain and KDR (data not shown). Taken together, these observations suggest that the extracellular domains of ECSCR and KDR are dispensable for their interaction in transfected cells.

We next compared ECSCR to a similarly sized endothelial glycoprotein, EMCN with respect to KDR co-IP (Fig. 2). In transfected HEK293 cells, ECSCR but not EMCN immunopre-

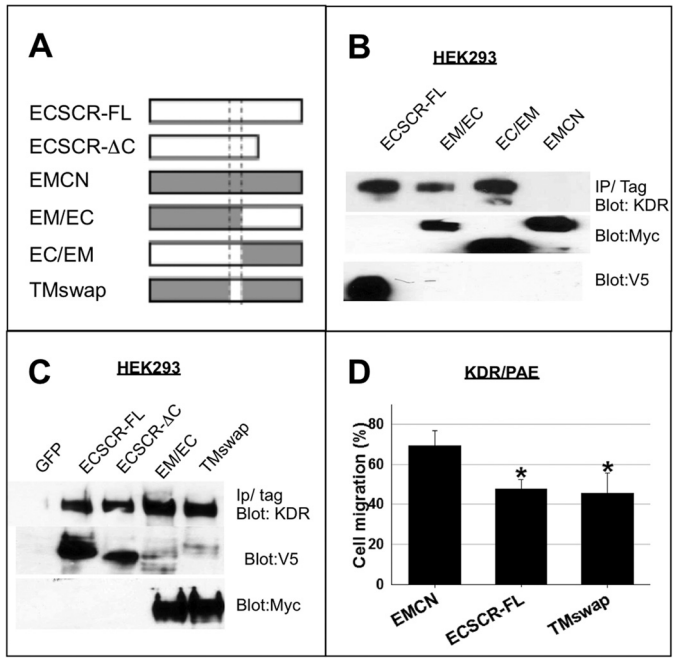

FIGURE 2. **Structure/function comparison of ECSCR and EMCN for KDR association.** *A*, schematic (not to scale) of constructs tested for co-immunoprecipitation with KDR. ECSCR-derived sequences are indicated with *white rectangles*; EMCN-derived sequences are indicated with *gray rectangles*. Annotated transmembrane regions are indicated by *vertical dashed lines*. *B*, ECSCR, but not EMCN, co-immunoprecipitates with KDR, whereas chimeric constructs EM/EC and EC/EM both associate with KDR. *C*, TMswap construct substituting ECSCR transmembrane region into EMCN confers KDR association. *D*, ECSCR overexpression impairs Boyden chamber migration of KDR/PAE relative to EMCN control. KDR/PAE cells were transfected with indicated constructs, starved, seeded into the top chamber of Transwell inserts and allowed to migrate in response to 20 ng/ml VEGF for 4 h. ECSCR- or TMswap-overexpressing cells showed reduced VEGF-stimulated Transwell migration compared with EMCN control. Results presented are the average of four independent experiments. *, $p < 0.05$, Student's *t* test.

cipitated with KDR (Fig. 2*B*). To better understand which regions of ECSCR mediate association with KDR, we generated recombinant constructs specifying chimeric proteins composed of ECSCR- and EMCN-derived sequences (schematically shown in Fig. 2*A*; see "Experimental Procedures" for details). We assayed the ECSCR extracellular and transmembrane domains combined with EMCN cytoplasmic tail (EC/EM) or, conversely, the EMCN extracellular and transmembrane domains with ECSCR cytoplasmic tail (EM/EC) for co-immunoprecipitation with KDR. Both EC/EM and EM/EC co-immunoprecipitated with KDR in this assay, indicating that more than one region of ECSCR can contribute to co-IP in this transfection system (Fig. 2*C*). To test whether ECSCR transmembrane sequences are sufficient for KDR co-IP, we expressed a chimeric EMCN-derived protein containing only the ECSCR transmembrane domain (TMswap; Fig. 2*A*). TMswap also immunoprecipitated with KDR (Fig. 2*C*). Finally, to test the functional consequences of KDR-ECSCR association for cellular responses to VEGF, we performed Boyden chamber analysis of KDR/PAE cells overexpressing control EMCN, ECSCR, or the TMswap (Fig. 2*D*). Overexpression of ECSCR or TMswap significantly reduced KDR/PAE migration toward VEGF relative to EMCN. Taken together, these findings show that ECSCR and KDR have a mutually selective biochemical association, and that sequences near or within the transmembrane domain of both KDR and ECSCR can contribute to this interaction. The data also support the possibility of ECSCR cytoplasmic sequences contributing to KDR association.

VEGF Stimulation Transiently Increases ECSCR-KDR Interaction—We next investigated whether VEGF stimulation affected ECSCR association with KDR. HUVECs were serum-starved overnight and then stimulated with $VEGF_{165}$ (25 ng/ml) for intervals ranging from 0 to 30 min (Fig. 3 and supplemental Fig. 1). Endogenous ECSCR/KDR co-immunoprecipitation was weak in starved cells and was strongly enhanced following 10 min of VEGF stimulation (Fig. 3*A*). Association levels returned to basal levels following 30 min (supplemental Fig. 1*A*). The time course of co-immunoprecipitation appeared to lag behind that of receptor activation, as assayed by KDR phosphorylation on tyrosine 951 (Ref. 23 and supplemental Fig. 1*A*). VEGF-stimulated co-IP was completely blocked by SU5416 (supplemental Fig. 1*A*). Stimulation with $VEGF_{121}$ provoked only a modest increase in ECSCR/KDR co-IP despite robust receptor activation (Fig. 3*B*). $VEGF_{165}$-enhanced co-IP of endogenous ECSCR and KDR was observed in a second cell type, the immortalized endothelioma line bEND.3 (supplemental Fig. 1*B*).

To test whether VEGF stimulated ECSCR/KDR co-IP required intracellular trafficking, we used the endosomal maturation inhibitors bafilomycin-A1 and chloroquine (Fig. 3*C*) as well as NH_4Cl (data not shown). Intriguingly, these inhibitors blocked the VEGF-stimulated increase in ECSCR/KDR co-IP, suggesting that sorting of internalized KDR and/or ECSCR was required for enhanced complex formation.

Intracellular ECSCR and KDR Co-localize in VEGF-stimulated HUVECs—Where in VEGF-stimulated cells do ECSCR and KDR interact? In differential centrifugation experiments, we observed that endogenous ECSCR and KDR are detected in serum-starved and VEGF-stimulated cells in both low-speed and high-speed pellets (enriched in plasma membrane and endosome material, respectively). However, we did not observe a correlation between subcellular fraction localization of ECSCR and KDR following VEGF stimulation (supplemental Fig. 2). We therefore attempted to identify the subcellular locus of interaction using immunocytochemical approaches (Fig. 4). We treated HUVECs overexpressing tagged ECSCR with $VEGF_{165}$ or $VEGF_{165}$ plus SU5416 as above. Cells were then fixed and immunostained for anti-tag, anti-KDR, and anti-NRP1 (Fig. 4 A-C). Untreated cells did not show noticeable co-localization of these three antigens (Fig. 4*A*). However, following 10 min of stimulation with $VEGF_{165}$, HUVECs displayed prominent NRP1/ECSCR/KDR co-localization in perinuclear vesicle-like structures. This co-localization was not detected in cells treated with VEGF plus SU5416 (Fig. 4*C*), corresponding with the co-immunoprecipitation results obtained with endogenous proteins. To further identify the cellular locus of ECSCR/KDR co-localization, we immunostained VEGF-treated cells using markers for intracellular compartments. The perinuclear immunoreactivity for ECSCR/KDR in VEGF-stimulated cells was partially immunopositive for HRS, a component of the ESCRT complex implicated in trafficking of ubiquitinated activated receptors (10). ECSCR/KDR co-localizing structures were frequently adjacent to, but did not coincide with, the degradative pathway marker RAB7, and they did not overlap with the recycling vesicle marker RAB11 (supplemental Fig. 3).

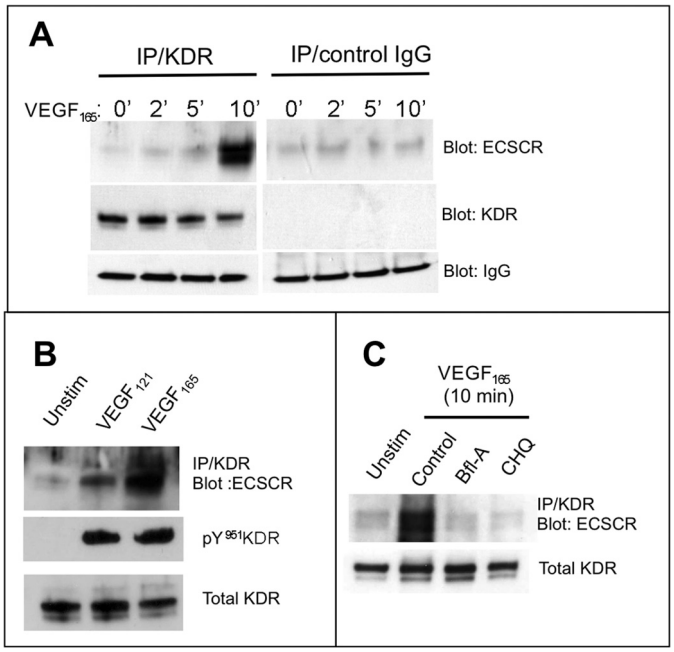

FIGURE 3. **Dynamic endogenous ECSCR-KDR association following VEGF stimulation.** Serum-starved HUVECs were treated with inhibitors then stimulated with VEGF as indicated. Cell lysates were analyzed by Western blot for total or activated KDR (as phosphotyrosine 951), or immunoprecipitated with anti-endogenous ECSCR and blotted with anti-endogenous KDR. Results presented are representative of at least three independent experiments. *A*, ECSCR-KDR co-IP is seen following 10 min of $VEGF_{165}$ stimulation. No ECSCR signal is seen in control immunoprecipitates. *B*, stimulation with $VEGF_{121}$ (25 ng/ml, 10 min) only elicits weak co-IP despite robust receptor activation. *C*, co-immunoprecipitation is blocked by the inhibitors of endosome acidification bafilomycin-A1 (*BflA*) or chloroquine (*CHQ*). *0′*, 0 min; *2′*, 2 min; *5′*, 5 min; *10′*, 10 min; *Unstim*, unstimulated.

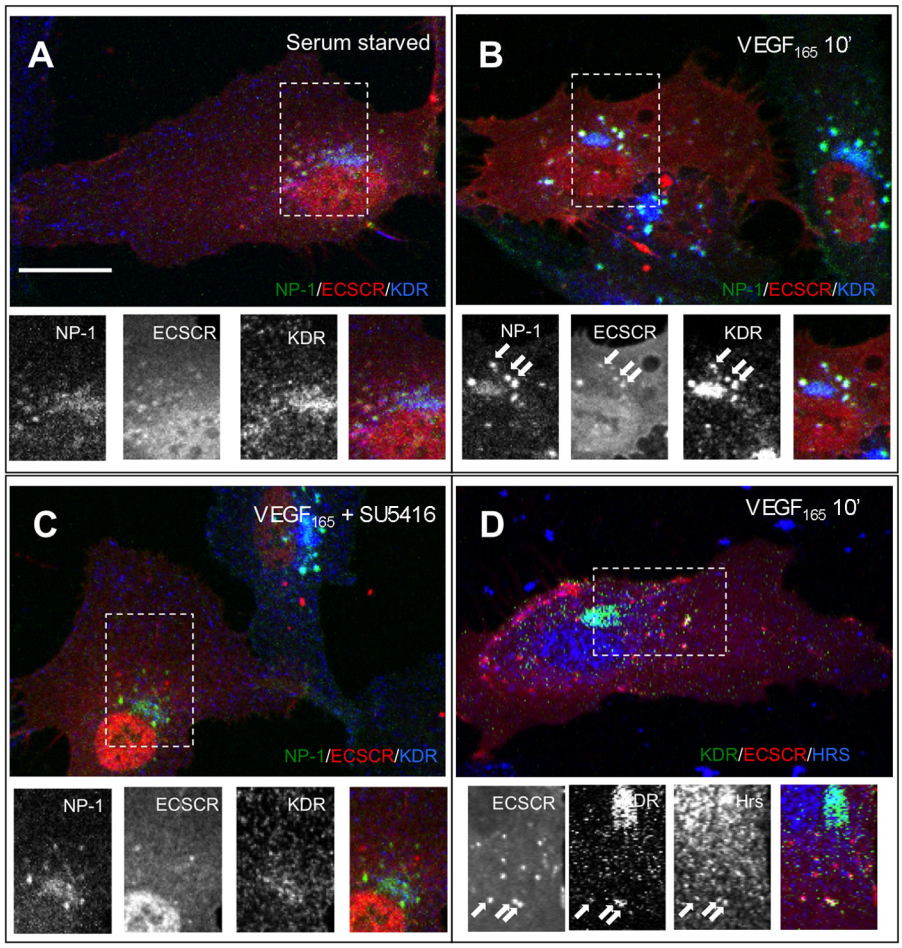

FIGURE 4. **KDR-ECSCR intracellular co-localization following VEGF stimulation.** HUVECs were microporated with ECSCR-FL, serum-starved, and then stimulated with VEGF or VEGF plus inhibitor as indicated. Cells were fixed and examined by confocal immunocytochemistry for ECSCR (as anti-tag), KDR, and either NRP1 or HRS. Results presented are representative of at least 10 cells from two independent microporations. Areas enclosed by *dashed boxes* in the larger *panels* are shown in single-channel breakouts below. *A*, serum-starved cell immunostained for NRP1 (*green*), ECSCR-FL (*red*), and KDR (*blue*) shows minimal co-localization of all three antigens. *Scale bar* for all large panels, 10 mm. *B*, after 10 min of VEGF stimulation, corresponding to maximum co-IP in biochemical experiments, NRP1/ECSCR/KDR triple co-localization is detected in perinuclear structures with vesicular appearance. *C*, NRP1/ECSCR/KDR triple co-localization is not detected when KDR activation is inhibited using SU5416. *D*, KDR/ECSCR double-immunopositive perinuclear vesicles show partial co-localization with the ESCRT-0 component HRS.

The co-localization of KDR and ECSCR with HRS prompted us to ask whether ECSCR might contribute to the proteolysis of activated KDR. We therefore stimulated control or ECSCR-silenced HUVECs with $VEGF_{165}$ and measured total KDR protein. Prolonged $VEGF_{165}$ stimulation of control cells elicited reduction of total KDR protein (9). In contrast, ECSCR-silenced cells showed attenuated proteolysis of KDR, with normalized KDR levels in ECSCR-silenced cells significantly elevated relative to control following 10 and 30 min of VEGF stimulation (Fig. 5*A*; quantified in Fig. 5*B*). Both total KDR (Fig. 5*B*) and surface KDR (Fig. 5*D*) were elevated following 10 min of VEGF stimulation.

We next investigated whether ECSCR overexpression would promote proteolysis of activated KDR. Surprisingly, HUVECs transfected with ECSCR-FL showed increased resting KDR protein levels (Fig. 5*C*). ELISA quantification showed an ~40% KDR protein increase in HUVECs overexpressing ECSCR-FL relative to control (data not shown). Quantitative real-time PCR measurements of *KDR* mRNA levels did not show significant differences following ECSCR transfection (data not shown). Because KDR in resting cells recycles between endosomes and the surface, we asked whether surface availability of KDR was affected by ECSCR overexpression. We treated HUVECs with the non-permeant biotinylation reagent Sulfo-NHS-biotin and subjected lysates to avidin pulldown and anti-KDR Western blot. HUVECs transfected with ECSCR showed a 30% increase in surface KDR (Fig. 5*C*, *top*, and data not shown). We also saw increased KDR protein levels in cells overexpressing the TMswap construct, suggesting that ECSCR protein-protein interactions affect KDR turnover in resting cells (data not shown). VEGF stimulation of ECSCR-FL overexpressing HUVECs did not show an increase in normalized KDR phosphorylation.

ECSCR Silencing Affects KDR Activation and AKT and ERK Phosphorylation—Receptor internalization and intracellular routing qualitatively alters signaling output (5). We therefore asked whether *ECSCR* silencing would affect downstream signals activated by VEGF signaling (Fig. 6*A*). HUVECs were transfected with control or *ECSCR*-silencing siRNAs, serum-starved, and stimulated with $VEGF_{165}$ for varying intervals.

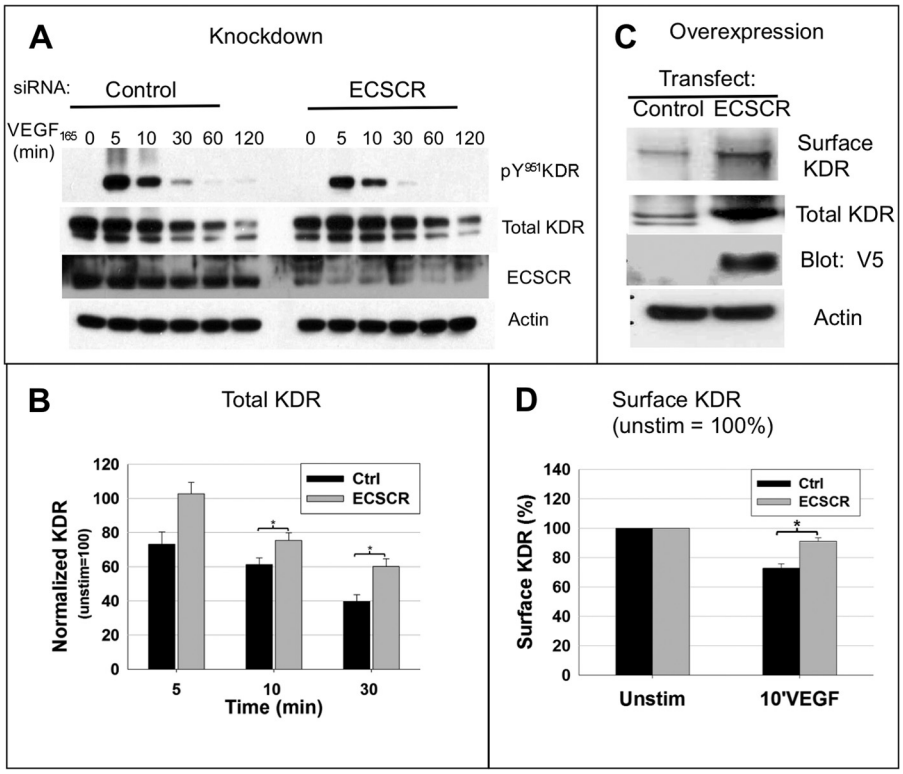

FIGURE 5. **Knockdown of ECSCR reduces VEGF-stimulated KDR proteolysis, whereas overexpression of ECSCR results in increased total and surface KDR protein.** *A*, HUVECs were transfected with control or *ECSCR* silencing siRNA and then subjected to extended VEGF stimulation. Total KDR and KDR phospho-Tyr^{951} were monitored by Western blot. ECSCR-deficient cells show increased KDR levels at 10 and 30 min, suggesting a reduced rate of VEGF-stimulated KDR degradation. *B*, densitometric quantification of KDR protein levels. Averaged KDR levels normalized to actin and to KDR signal in unstimulated cells, from at least four separate experiments employing two separate *ECSCR* targeting siRNAs. *C*, HUVECs transfected with ECSCR-FL display increased total KDR relative to control. This increase also is reflected in surface-biotinylatable KDR (*top panel*). *D*, ECSCR-silenced cells show significantly increased surface KDR relative to control. Flow cytometric analysis of surface KDR in control and ECSCR-silenced cells in serum-starved and VEGF-stimulated pools. Results represent the average of three independent experiments. *, $p < 0.05$, Student's *t* test. *Ctrl*, control; *Unstim*, unstimulated.

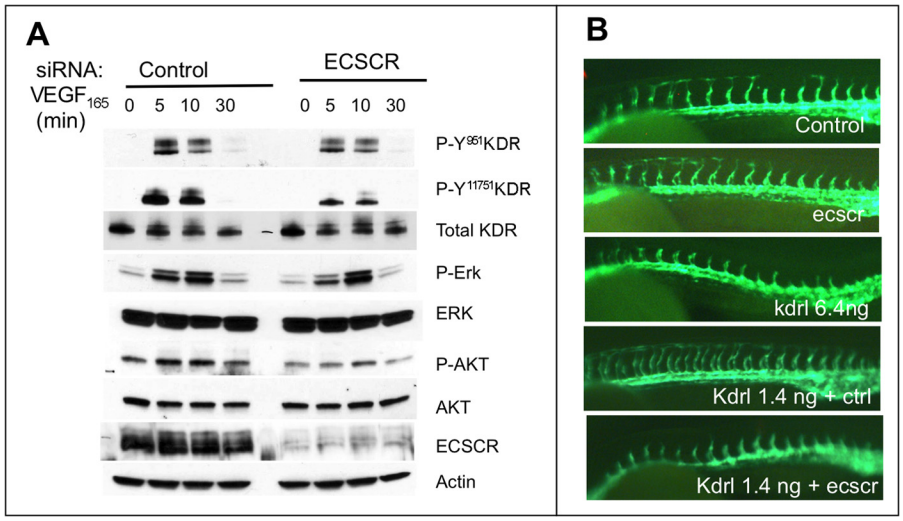

FIGURE 6. **Loss of ECSCR reduces early KDR activation and downstream signals and morpholino targeting of *ecscr* increases penetrance of subefficaceous *kdrl* targeting during zebrafish intersomitic vessel sprouting.** *A*, Western blot analysis of KDR activation and AKT and ERK phosphorylation following VEGF stimulation of control and *ECSCR*-silenced HUVECs. Inactivation of *ECSCR* results in receptor hypoactivity, delay of ERK phosphorylation peak, and reduced basal and VEGF-stimulated AKT phosphorylation. Results are representative of three independent experiments employing two separate *ECSCR* siRNAs and are quantified in supplemental Fig. 3. *B*, whole mount photomicrographs of *kdrl*:*GFP* transgenic zebrafish embryos following injection of the indicated morpholinos. Injection of ecscr targeting morpholino, or 1.4 ng of *kdrl*-targeting morpholino, does not impair ISV sprouting. However, injection of both together results in visibly delayed sprouting in 88% of embryos relative to controls (*ctrl*).

Cells lysates were analyzed for phosphorylation of KDR and downstream signaling proteins AKT and ERK. Consistent our earlier observations (1), *ECSCR*-silenced HUVECs showed reduced VEGF-induced KDR phosphorylation on tyrosine 951 and showed a trend toward reduced phosphorylation on tyrosine 1175, at 5 min (Fig. 6*A*; quantification in supplemental Fig. 4). Extending

TABLE 1

Intersomitic vessel sprouting phenotypes in ECSCR loss of function zebrafish

Flk1:GFP transgenic zebrafish were injected with morpholinos as indicated and scored at 22 hpf for intersomitic vessel sprouting by an observer blind to injection conditions. Results presented are total number scored and number and percentage of embryos with visibly delayed intersomitic vessel sprouting. (Significant differences of observed distributions are indicated as follows: ***, $p < 0.001$ *versus* ECSCR MO injected.)

Injection	No. scored	No. abnormal	Percent abnormal
Control MO	26	0	0.00
kdrl (6.4 ng)	44	44	100.00***
kdrl (3.2 ng)	16	8	50.00***
kdrl (1.4 ng)	12	2	16.67
kdrl (1.4 ng) + *ecscr (6.4 ng)*	75	66	88.00***
kdrl (1.4 ng) + cMO (6.4 ng)	12	1	8.33
ecscr (6.4 ng)	25	1	4.00

the observation of KDR hypoactivity, we also observed reductions in phosphorylation of Akt (Ser^{473}) and ERK (p42/44). Anti-phospho-Akt showed reduced signals in basal and VEGF-stimulated cells. Anti-phospho-ERK analysis showed delayed and blunted peak signal.

Ecscr Morpholino Exacerbates ISV Sprouting Angiogenesis Delay in Zebrafish Injected with Subefficaceous Dose of kdrl Targeting Morpholino—To determine whether *ecscr* interacts with VEGF receptors in zebrafish, we evaluated ISV sprouting, which requires full function of the VEGF receptor *kdrl* (18, 24). At 22 hpf, 100% of Tg(*kdrl:EGFP*) zebrafish injected with 6.4 ng of *kdrl* MO showed delayed ISV sprouting relative to control (Ref. 18 and Table 1). We next injected successively lower dosages of *kdrl* MO and determined that injection of 1.4 ng resulted in minimal incidence of ISV sprouting delay (Table 1). We thus chose this dosage as a sensitizing dosage to be evaluated in combination with *ecscr* MO. We coinjected 1.4 ng of *kdrl* MO along with 6.4 ng, an inactivating dosage, of *ecscr* MO (1) or control MO, and compared the ISV system in each sample (Table 1 and Fig. 6*B*). ISVs of embryos singly injected with 6.4 ng of *ecscr* MO or with the sensitizing dosage 1.4 ng of *kdrl* MO had completed their dorsal trajectory and begun bifurcation. In contrast, embryos injected with full dosage, 6.4 ng of *kdrl* MO, or coinjected with 1.4 ng of *kdrl* MO plus 6.4 ng of *ecscr* MO, showed delay of ISV extension (Table 1 and Fig. 6*B*). Embryos coinjected with 1.4 ng of *kdrl* MO plus control MO resembled control groups (Fig. 6*B*).

ECSCR Expression in Human Placenta and Proliferative Stage Infantile Hemangioma— Although the tissue distribution of *ECSCR* mRNA has been extensively characterized (1, 11, 14, 25, 26), the distribution of ECSCR protein *in vivo* is largely unknown. To investigate this and to identify the potential *in vivo* significance of the ECSCR-KDR interaction, we utilized our anti-ECSCR antiserum to screen a human cardiovascular disease tissue array for ECSCR protein expression (results presented in supplemental Table 1 and supplemental Fig. 5). Strong ECSCR immunoreactivity was detected in healthy tissue samples from major vessels, myocardium, placenta, and spleen. Strong expression was also seen in several disease samples, including liver hemangioma, carotid body paraganglioma, nasal cavity angioleiomyoma, and skin ulcer granulation tissue. We selected human placenta for further analysis (Fig. 7). In placenta, we detected strong ECSCR immunoreactivity in extravillar trophoblasts within the basal plate (Fig. 7*A*) and microvessels within the myometrium (Fig. 7*B*). Marker analysis confirmed that $ECSCR^+$ cells in the basal plate were positive for the invasive trophoblast marker cytokeratin 7 (Fig. 7*C*) and negative for the microvascular antigen CD34 (Fig. 7*D*). Because placental trophoblasts and endothelial cells of vascular tumor hemangioma share markers and possibly a common developmental origin (27), we next investigated whether ECSCR protein expression was altered in biopsies from patients with infantile hemangioma. Western blot analysis showed elevated ECSCR protein in proliferating phase hemangioma samples relative to early stage (Fig. 7*C*). Immunostaining of hemangioma cryostat sections showed ECSCR immunoreactivity over both pathological, Glut-1-positive vasculature (28) and adjacent

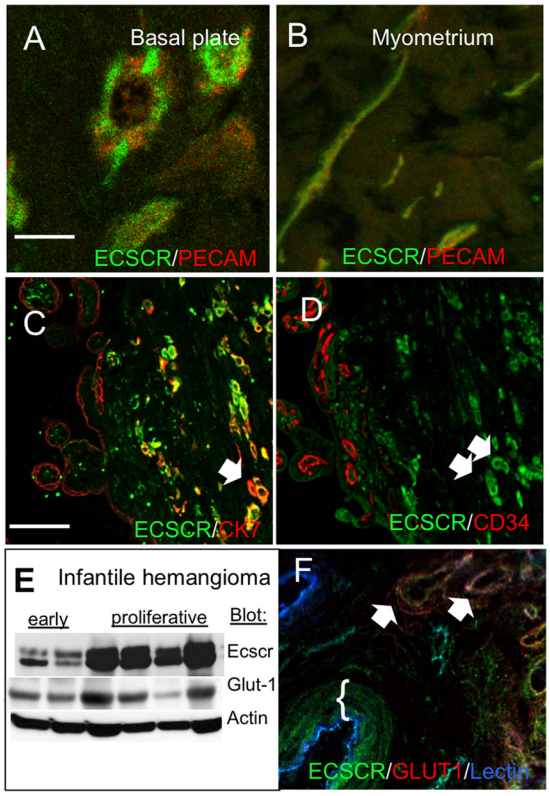

FIGURE 7. **ECSCR protein distribution in human placenta and infantile hemangioma.** *A* and *B*, double labeled confocal photomicrograph of sections of human placental basal plate (*A*) and myometrium (*B*) labeled with anti-ECSCR (*green*) and anti-PECAM-1 (*red*). Prominent ECSCR immunoreactivity is detected on placental bed extravillous trophoblasts and on the myometrium vasculature. *Scale bar* for *A* and *B*, 5 μm. *C* and *D*, marker analysis of ECSCR immunoreactivity in human placenta. Survey double labeled confocal photomicrograph of human placenta near the fetal-maternal interface. Placenta is stained with anti-ECSCR (*green*) and anti-cytokeratin 7, a marker for epithelial cells including trophoblasts (cytokeratin 7; *CK7*; *C*); and with anti-ECSCR and anti-CD34, a marker for microvessels (*D*). ECSCR immunoreactivity is seen on $CK7^+$, $CD34^-$ invasive trophoblasts (*arrows*). *Scale bar* for *C* and *D*, 100 μm. *E*, Western blot analysis of ECSCR, hemangioma EC marker GLUT-1, and β-actin reference in tissue lysates of early-stage and proliferative stage infantile hemangioma. ECSCR protein levels are strongly elevated in biopsies from proliferative stage hemangioma. *F*, triple-labeled confocal photomicrograph of a section through a proliferative stage hemangioma, labeled for ECSCR (*green*), GLUT-1 (*red*), and for the general endothelial marker Ulex-1 lectin (*blue*). ECSCR positivity is seen on vessels immunopositive for Glut-1^+ (*arrowheads*) as well as microvessels negative for Glut-1. ECSCR immunoreactivity is also seen in the perivascular tissue (*white bracket*) of a non-diseased artery.

normal vasculature (Fig. 7*D*). We also observed ECSCR immunoreactivity in the perivascular tissue surrounding the normal artery, which may reflect previously reported vascular smooth muscle cell expression (14). Finally, we confirmed strong KDR co-expression with ECSCR on the characteristic plump endothelial cells lining tumor microvessels (supplemental Fig. 5*H*). Taken together, these results suggest dysregulation of ECSCR in during the proliferative phase of this disorder.

ECSCR Message and Endothelial Protein Is Reduced in Lung Solid Tumors—To examine changes in ECSCR in disease, we examined ECSCR message and protein expression in lung, a highly vascularized tissue expressing high levels of *ECSCR* mRNA in the healthy state (25). Quantitative PCR measurements showed that *ECSCR* transcript was strongly reduced in squamous cell carcinoma and adenocarcinoma biopsies relative to healthy lung (supplemental Fig. 6*A*). Similarly, protein samples from lung squamous cell carcinoma in mice following treatment with with *N*-nitroso-tris-chloroethylurea (reviewed in Ref. 29) showed consistent reduction in ECSCR protein, even when normalized to PECAM-1 endothelial reference. Anti-ECSCR immunostain comparison of healthy lung and lung squamous cell carcinoma tissue showed that ECSCR is present on multiple cell types, including microvessels in healthy lung. In contrast, ECSCR immunoreactivity is almost undetectable in tumor microvessels in disease samples (supplemental Fig. 6*D*).

DISCUSSION

We have show mutually selective biochemical association between ECSCR and KDR and identified the transmembrane and cytoplasmic regions of ECSCR and KDR as important for this association in transfected cells. Endogenous ECSCR/KDR association is increased by $VEGF_{165}$ stimulation, with complex formation observed at 10 min, and basal levels seen after 30 min. The time course of VEGF-stimulated ECSCR-KDR complex formation; the sensitivity of the effect to bafilomycin-A and chloroquine; the location of $ECSCR^+/KDR^+$ immunoreactivity in vesicles marked by HRS; and the phenotype of ECSCR silenced cells all suggest that ECSCR interacts transiently with activated KDR in an internal cellular compartment. The observations that ECSCR-KDR coIP is detected following stimulation with VEGF165, not VEGF121, and that ECSCR-KDR co-localizes with NRP1, both suggest a role for NRP1 in the stimulated ECSCR-KDR complex formation. The nature of the NRP1 role remains obscure but could involve formation of a multiprotein complex or differential routing of KDR via NRP1 cytoplasmic interactors (5).

The relationship between basal co-immunoprecipitation seen in resting cells and the strong increase seen following VEGF stimulation remains uncertain at this point. Because early KDR signaling is impaired in ECSCR silenced cells, we speculate that basal ECSCR/KDR complexes are located at or near the cell surface, where ECSCR enhances KDR activation with short latency. In contrast, VEGF-elicited ECSCR-KDR complexes form slowly compared with KDR tyrosine phosphorylation are blocked by inhibitors of receptor activation or endosomal acidification. We would speculate that these complexes act to promote KDR degradation upstream of RAB7 and possibly RAB11 compartments. By comparison, complex formation between KDR and NRP1 is also detected soon after VEGF stimulation but is sustained for much longer periods (30) with this complex preferentially directed toward the RAB11 slow recycling pathway. In our earlier analysis of freely growing HUVECs (1), we saw co-localization of KDR and ECSCR at the surface of protrusive lamellar processes. We would speculate that this basal cell-surface association is disrupted following VEGF stimulation and then followed by internalization and intracellular reassociation. Alternatively, separate subcellular pools of ECSCR could bind KDR independent of ECSCR trafficking.

Together with the structure/function analysis performed in resting cells, these observations shed light on the selective impact on tyrosine phosphorylation of KDR but not FLT1 in ECSCR-silenced cells (1) and suggest a broad mechanism for ECSCR to modulate KDR-dependent cellular responses. Additional work would be required to understand the relationship between basal and VEGF-dependent ECSCR-KDR complexes and the internalization route(s) taken by the two component proteins prior to enhanced complex formation.

KDR, the Hub of a Versatile Cell-surface Protein Network—It is becoming increasingly clear that KDR surface availability, activation, and trafficking are all affected by cell-surface molecules not directly implicated with the growth factor binding site (reviewed in Ref. 31). ECSCR joins this group along with the junctional protein VE-cadherin (32), the seven-transmembrane domain protein dopamine type 2 receptor (33), and the Eph receptor ligand ephrin-B2 (34, 35). Our screen of ECSCR protein distribution showed vascular ECSCR in a number of normal and disease tissues. Of interest, ECSCR was highly expressed by extravillous trophoblasts in placenta. KDR is prominently expressed by placental trophoblasts throughout pregnancy (36), and dysregulation of VEGF signaling is implicated in the etiology of numerous vascular anomalies including infantile hemangioma (37). We found prominent ECSCR protein expression in both these contexts, suggesting that the ECSCR-KDR protein module may be dysregulated in this disease. In other contexts, such as lung solid tumors, ECSCR protein levels appear to be very low. ECSCR may interact differentially with diverse cell-surface proteins to elicit vascular bed-specific KDR endothelial responses and could be used as drug targets to influence KDR activation in select endothelial cells.

Distinct Impact of ECSCR Silencing and Overexpression—The precise impact of ECSCR gain or loss of function may depend on context in a manner that remains poorly understood (reviewed in Ref. 16). For example, loss of ECSCR has resulted in differential impact on EC migration, depending on stimulus, cell type, and assay conditions (1, 11, 13, 14). Our earlier (1) and current observations indicate that loss and gain of ECSCR can both result in decreased VEGF-dependent migration. Although both experimental manipulations impaired migration, gain and loss of function of ECSCR resulted in distinct effects upon KDR protein levels. ECSCR-silenced cells consistently showed reduced VEGF-stimulated KDR proteolysis of KDR, whereas ECSCR overexpressing cells showed increased basal KDR protein but no appreciable reduction in VEGF-stimulated proteolysis (Fig. 5 and data not shown). One scenario encompassing both sets of biochemical data and resultant migratory phenotypes would emphasize the impor-

tance of internalization processes in a directional migratory response. Receptor trafficking influences the targets and duration of downstream signaling (38), and the reduced KDR signaling coupled with delayed proteolysis seen in ECSCR-deficient cells may explain the impairment of migration in those cells. Conversely, the increased surface presentation of KDR seen in ECSCR overexpressing cells could result in cell hypersensitivity, blunting directionality of the migratory response (39).

In conclusion, we have clarified the mechanism by which ECSCR affects KDR activation and VEGF responses in ECs. ECSCR forms a complex with the VEGF-stimulated receptor, affecting KDR tyrosine phosphorylation, proteolysis, and activation of downstream signals. ECSCR protein expression in proliferating stage human infantile hemangioma has potential implications for control of this neoplasm.

Acknowledgments—We thank the members of the Children's Research Institute Imaging and Histology Core for advice and assistance in immunohistochemistry.

REFERENCES

1. Verma, A., Bhattacharya, R., Remadevi, I., Li, K., Pramanik, K., Samant, G. V., Horswill, M., Chun, C. Z., Zhao, B., Wang, E., Miao, R. Q., Mukhopadhyay, D., Ramchandran, R., and Wilkinson, G. A. (2010) Endothelial cell-specific chemotaxis receptor (ecscr) promotes angioblast migration during vasculogenesis and enhances VEGF receptor sensitivity. *Blood* **115,** 4614–4622
2. Soker, S., Miao, H. Q., Nomi, M., Takashima, S., and Klagsbrun, M. (2002) VEGF165 mediates formation of complexes containing VEGFR-2 and neuropilin-1 that enhance VEGF165-receptor binding. *J. Cell Biochem.* **85,** 357–368
3. Pan, Q., Chathery, Y., Wu, Y., Rathore, N., Tong, R. K., Peale, F., Bagri, A., Tessier-Lavigne, M., Koch, A. W., and Watts, R. J. (2007) Neuropilin-1 binds to VEGF121 and regulates endothelial cell migration and sprouting. *J. Biol. Chem.* **282,** 24049–24056
4. Flynn, E. J., 3rd, Trent, C. M., and Rawls, J. F. (2009) Ontogeny and nutritional control of adipogenesis in zebrafish (*Danio rerio*). *J. Lipid Res.* **50,** 1641–1652
5. Horowitz, A., and Seerapu, H. R. (2012) Regulation of VEGF signaling by membrane traffic. *Cell Signal.* **24,** 1810–1820
6. Gampel, A., Moss, L., Jones, M. C., Brunton, V., Norman, J. C., and Mellor, H. (2006) VEGF regulates the mobilization of VEGFR2/KDR from an intracellular endothelial storage compartment. *Blood* **108,** 2624–2631
7. Ballmer-Hofer, K., Andersson, A. E., Ratcliffe, L. E., and Berger, P. (2011) Neuropilin-1 promotes VEGFR-2 trafficking through Rab11 vesicles thereby specifying signal output. *Blood* **118,** 816–826
8. Duval, M., Bédard-Goulet, S., Delisle, C., and Gratton, J. P. (2003) Vascular endothelial growth factor-dependent down-regulation of Flk-1/KDR involves Cbl-mediated ubiquitination. Consequences on nitric oxide production from endothelial cells. *J. Biol. Chem.* **278,** 20091–20097
9. Ewan, L. C., Jopling, H. M., Jia, H., Mittar, S., Bagherzadeh, A., Howell, G. J., Walker, J. H., Zachary, I. C., and Ponnambalam, S. (2006) Intrinsic tyrosine kinase activity is required for vascular endothelial growth factor receptor 2 ubiquitination, sorting and degradation in endothelial cells. *Traffic* **7,** 1270–1282
10. Haglund, K., and Dikic, I. (2012) The role of ubiquitylation in receptor endocytosis and endosomal sorting. *J. Cell Sci.* **125,** 265–275
11. Armstrong, L. J., Heath, V. L., Sanderson, S., Kaur, S., Beesley, J. F., Herbert, J. M., Legg, J. A., Poulsom, R., and Bicknell, R. (2008) ECSM2, an endothelial specific filamin a binding protein that mediates chemotaxis. *Arterioscler. Thromb. Vasc. Biol.* **28,** 1640–1646
12. Herbert, J. M., Stekel, D., Sanderson, S., Heath, V. L., and Bicknell, R. (2008) A novel method of differential gene expression analysis using multiple cDNA libraries applied to the identification of tumour endothelial genes. *BMC Genomics* **9,** 153
13. Shi, C., Lu, J., Wu, W., Ma, F., Georges, J., Huang, H., Balducci, J., Chang, Y., and Huang, Y. (2011) Endothelial cell-specific molecule 2 (ECSM2) localizes to cell-cell junctions and modulates bFGF-directed cell migration via the ERK-FAK pathway. *PLoS One* **6,** e21482
14. Ikeda, K., Nakano, R., Uraoka, M., Nakagawa, Y., Koide, M., Katsume, A., Minamino, K., Yamada, E., Yamada, H., Quertermous, T., and Matsubara, H. (2009) Identification of ARIA regulating endothelial apoptosis and angiogenesis by modulating proteasomal degradation of cIAP-1 and cIAP-2. *Proc. Natl. Acad. Sci. U.S.A.* **106,** 8227–8232
15. Kennedy, D. J., Kuchibhotla, S., Westfall, K. M., Silverstein, R. L., Morton, R. E., and Febbraio, M. (2011) A CD36-dependent pathway enhances macrophage and adipose tissue inflammation and impairs insulin signalling. *Cardiovasc. Res.* **89,** 604–613
16. Raldúa, D., André, M., and Babin, P. J. (2008) Clofibrate and gemfibrozil induce an embryonic malabsorption syndrome in zebrafish. *Toxicol. Appl. Pharmacol.* **228,** 301–314
17. Motoike, T., Loughna, S., Perens, E., Roman, B. L., Liao, W., Chau, T. C., Richardson, C. D., Kawate, T., Kuno, J., Weinstein, B. M., Stainier, D. Y., and Sato, T. N. (2000) Universal GFP reporter for the study of vascular development. *Genesis* **28,** 75–81
18. Bahary, N., Goishi, K., Stuckenholz, C., Weber, G., Leblanc, J., Schafer, C. A., Berman, S. S., Klagsbrun, M., and Zon, L. I. (2007) Duplicate VegfA genes and orthologues of the KDR receptor tyrosine kinase family mediate vascular development in the zebrafish. *Blood* **110,** 3627–3636
19. Garnaas, M. K., Moodie, K. L., Liu, M. L., Samant, G. V., Li, K., Marx, R., Baraban, J. M., Horowitz, A., and Ramchandran, R. (2008) Syx, a RhoA guanine exchange factor, is essential for angiogenesis *in vivo*. *Circ. Res.* **103,** 710–716
20. Chun, C. Z., Kaur, S., Samant, G. V., Wang, L., Pramanik, K., Garnaas, M. K., Li, K., Field, L., Mukhopadhyay, D., and Ramchandran, R. (2009) Snrk-1 is involved in multiple steps of angioblast development and acts via notch signaling pathway in artery-vein specification in vertebrates. *Blood* **113,** 1192–1199
21. Grünewald, F. S., Prota, A. E., Giese, A., and Ballmer-Hofer, K. (2010) Structure-function analysis of VEGF receptor activation and the role of coreceptors in angiogenic signaling. *Biochim. Biophys. Acta* **1804,** 567–580
22. Rahimi, N., Dayanir, V., and Lashkari, K. (2000) Receptor chimeras indicate that the vascular endothelial growth factor receptor-1 (VEGFR-1) modulates mitogenic activity of VEGFR-2 in endothelial cells. *J. Biol. Chem.* **275,** 16986–16992
23. Matsumoto, T., Bohman, S., Dixelius, J., Berge, T., Dimberg, A., Magnusson, P., Wang, L., Wikner, C., Qi, J. H., Wernstedt, C., Wu, J., Bruheim, S., Mugishima, H., Mukhopadhyay, D., Spurkland, A., and Claesson-Welsh, L. (2005) VEGF receptor-2 Y951 signaling and a role for the adapter molecule TSAd in tumor angiogenesis. *EMBO J.* **24,** 2342–2353
24. Leijh, P. C., van Zwet, T. L., ter Kuile, M. N., and van Furth, R. (1984) Effect of thioglycolate on phagocytic and microbicidal activities of peritoneal macrophages. *Infect. Immun.* **46,** 448–452
25. Ma, F., Zhang, D., Yang, H., Sun, H., Wu, W., Gan, Y., Balducci, J., Wei, Y. Q., Zhao, X., and Huang, Y. (2009) Endothelial cell-specific molecule 2 (ECSM2) modulates actin remodeling and epidermal growth factor receptor signaling. *Genes Cells* **14,** 281–293
26. Koide, M., Ikeda, K., Akakabe, Y., Kitamura, Y., Ueyama, T., Matoba, S., Yamada, H., Okigaki, M., and Matsubara, H. (2011) Apoptosis regulator through modulating IAP expression (ARIA) controls the PI3K/Akt pathway in endothelial and endothelial progenitor cells. *Proc. Natl. Acad. Sci. U.S.A.* **108,** 9472–9477
27. North, P. E., Waner, M., Mizeracki, A., Mrak, R. E., Nicholas, R., Kincannon, J., Suen, J. Y., and Mihm, M. C., Jr. (2001) A unique microvascular phenotype shared by juvenile hemangiomas and human placenta. *Arch. Dermatol.* **137,** 559–570
28. North, P. E., Waner, M., Buckmiller, L., James, C. A., and Mihm, M. C., Jr. (2006) Vascular tumors of infancy and childhood: beyond capillary hemangioma. *Cardiovasc. Pathol.* **15,** 303–317
29. You, M. S., Rouggly, L. C., You, M., and Wang, Y. (2012) *Cancer Metastasis Rev.* DOI 10.1007/s10555-012-9406-4

30. Prahst, C., Héroult, M., Lanahan, A. A., Uziel, N., Kessler, O., Shraga-Heled, N., Simons, M., Neufeld, G., and Augustin, H. G. (2008) Neuropilin-1-VEGFR-2 complexing requires the PDZ-binding domain of neuropilin-1. *J. Biol. Chem.* **283,** 25110–25114
31. Eichmann, A., and Simons, M. (2012) VEGF signaling inside vascular endothelial cells and beyond. *Curr. Opin. Cell Biol.* **24,** 188–193
32. Carmeliet, P., Lampugnani, M. G., Moons, L., Breviario, F., Compernolle, V., Bono, F., Balconi, G., Spagnuolo, R., Oosthuyse, B., Dewerchin, M., Zanetti, A., Angellilo, A., Mattot, V., Nuyens, D., Lutgens, E., Clotman, F., de Ruiter, M. C., Gittenberger-de Groot, A., Poelmann, R., Lupu, F., Herbert, J. M., Collen, D., and Dejana, E. (1999) Targeted deficiency or cytosolic truncation of the VE-cadherin gene in mice impairs VEGF-mediated endothelial survival and angiogenesis. *Cell* **98,** 147–157
33. Sinha, S., Vohra, P. K., Bhattacharya, R., Dutta, S., Sinha, S., and Mukhopadhyay, D. (2009) Dopamine regulates phosphorylation of VEGF receptor 2 by engaging Src-homology-2-domain-containing protein tyrosine phosphatase 2. *J. Cell Sci.* **122,** 3385–3392
34. Sawamiphak, S., Seidel, S., Essmann, C. L., Wilkinson, G. A., Pitulescu, M. E., Acker, T., and Acker-Palmer, A. (2010) Ephrin-B2 regulates VEGFR2 function in developmental and tumour angiogenesis. *Nature* **465,** 487–491
35. Wang, Y., Nakayama, M., Pitulescu, M. E., Schmidt, T. S., Bochenek, M. L., Sakakibara, A., Adams, S., Davy, A., Deutsch, U., Lüthi, U., Barberis, A., Benjamin, L. E., Mäkinen, T., Nobes, C. D., and Adams, R. H. (2010) Ephrin-B2 controls VEGF-induced angiogenesis and lymphangiogenesis. *Nature* **465,** 483–486
36. Clark, D. E., Smith, S. K., Sharkey, A. M., and Charnock-Jones, D. S. (1996) Localization of VEGF and expression of its receptors flt and KDR in human placenta throughout pregnancy. *Hum. Reprod.* **11,** 1090–1098
37. Jinnin, M., Medici, D., Park, L., Limaye, N., Liu, Y., Boscolo, E., Bischoff, J., Vikkula, M., Boye, E., and Olsen, B. R. (2008) Suppressed NFAT-dependent VEGFR1 expression and constitutive VEGFR2 signaling in infantile hemangioma. *Nat. Med.* **14,** 1236–1246
38. Rainero, E., and Norman, J. C. (2011) New roles for lysosomal trafficking in morphogen gradient sensing. *Sci. Signal* **4,** pe24
39. Jékely, G., Sung, H. H., Luque, C. M., and Rørth, P. (2005) Regulators of endocytosis maintain localized receptor tyrosine kinase signaling in guided migration. *Dev. Cell* **9,** 197–207